AIP | The Journal of Chemical Physics

Density functional theory study of β -hydride elimination of ethyl on flat and stepped Cu surfaces

Xin Li, Andrew J. Gellman, and David S. Sholl

Citation: The Journal of Chemical Physics **127**, 144710 (2007); doi: 10.1063/1.2786994
View online: http://dx.doi.org/10.1063/1.2786994
View Table of Contents: http://scitation.aip.org/content/aip/journal/jcp/127/14?ver=pdfcov
Published by the AIP Publishing

Density functional theory study of β-hydride elimination of ethyl on flat and stepped Cu surfaces

Xin Li
Department of Chemistry, Carnegie Mellon University, Pittsburgh, Pennsylvania 15213, USA

Andrew J. Gellman and David S. Sholl[a)]
Department of Chemical Engineering, Carnegie Mellon University, Pittsburgh, Pennsylvania 15213, USA

(Received 4 April 2007; accepted 28 August 2007; published online 11 October 2007)

Plane wave density functional theory calculations have been used to characterize the transition states for β-hydride elimination of ethyl on Cu(100), Cu(110), Cu(111), and Cu(221). The reaction rates predicted by these calculations have been compared to experiments by including tunneling corrections within harmonic transition state theory. Tunneling corrections are found to be important in describing the peak temperatures observed using temperature programed desorption experiments on Cu(110), Cu(111), and Cu(221). Once these corrections are included, the effective activation energies obtained from our calculations are in good agreement with previous experimental studies of this reaction on these four Cu surfaces. The transition states determined in our calculations are used to examine two general hypotheses that have been suggested to describe structure sensitivity in metal-catalyzed surface reactions. © *2007 American Institute of Physics*.
[DOI: 10.1063/1.2786994]

I. INTRODUCTION

The dehydrogenation of ethyl is an important elementary step in surface chemistry. A detailed understanding of the mechanism of such elementary processes is of great importance to help understand the corresponding catalytic processes.[1–5] The ethyl group tends to be unstable on most transition metal surfaces, so it can be challenging to obtain experimental data on its reaction mechanism. Jenks *et al.* have generated ethyl fragments on different low index Cu surfaces from ethyl iodides.[6,7] During the subsequent reaction step, the ethyl group decomposes into ethylene through the β-hydride elimination mechanism. β-hydride elimination reactions have also been investigated by Gellman and Dai in studies of the decomposition of alkyl groups into alkenes on Cu(111).[8,9] In this work, substituent effects were used to examine propyl groups on Cu(111) surfaces, resulting in the conclusion that the transition state for β-hydride elimination is cationic relative to the initial adsorbed species.

Experimental studies have provided information about the structure sensitivity of β-hydride elimination of ethyl on Cu surfaces by systematically comparing reaction properties on several single crystal surfaces. Jenks *et al.* used temperature programed desorption (TPD) to characterize the thermal chemistry of iodoethane on different Cu surfaces.[6] β-hydride elimination was found to be the rate-limiting step, and this reaction was significantly faster on Cu(110) than on either Cu(100) or Cu(111). Sung and Gellman have measured the kinetics of β-hydride elimination reaction of ethyl on Cu(111) and Cu(221),[10] which has a (111) terrace separated by (110) steps, by depositing ethyl iodide on these surfaces. On both surfaces, the first reaction step is the decomposition of the ethyl iodide, followed by the β-hydride elimination of the ethyl group into ethylene. The desorption rate of the ethylene was measured via TPD. The kinetics of the β-hydride elimination of ethyl on Cu(221) (Ref. 10) was found to be similar to the β-hydride elimination of ethyl on the Cu(110).[6] This observation is somewhat surprising when compared to the usual expectation that the presence of surface step edges will enhance the reactivity of a surface.

Over the past ten years, density functional theory (DFT) has been widely used to analyze the reaction mechanism of the β-hydride elimination of alkyl groups on metal surfaces. Using DFT, Wang *et al.* have studied the adsorption of methyl on the (111) surfaces of some transition and noble metal surfaces M (M=Cu, Ni, Rh, Pt, Pd, Ag, and Au) and on Fe(100).[11] The hollow site is found to be more stable than atop site on Fe, Ni, Rh, and Cu, while the atop site is more stable on Pt, Pd, Au, and Ag. Ciobica *et al.* have used DFT to study the C—H activation of methyl on Ru(0001), and the activation energy was determined to be 0.51 eV.[12] Gong *et al.* and Michaelides and Hu used DFT to study the reverse reaction, namely, hydrogenation of CH_2 on different metal surfaces, such as Ni(111), Pd(100), Pt(111), and Co(0001).[3,13–15] The calculated energy barriers to CH_2 hydrogenation are below 1 eV, consistent with experimental work. Recently, Truhlar and Morokuma used DFT to compute the activation energy barrier of β-hydride elimination of ethyl, CH_3CH_2–, on Pd (111) to be 0.72 eV.[16] Experimentally, this barrier was measured to be 0.41–0.59 eV by Kovacs and Solymosi.[17] Truhlar and Morokuma also studied β-hydride elimination of fluorinated ethyl, CFH_2CH_2–, and found some similarities in the calculated geometry of the transition states between fluorinated ethyl and ethyl, assuming that the reaction mechanism is not altered by fluorination.

[a)]Author to whom correspondence should be addressed. Electronic mail: sholl@andrew.cmu.edu

Applying DFT to characterize the transition states for a set of surface reactions provides an opportunity to test a general hypothesis that has been put forward to determine when surface reactions are structure sensitive. This hypothesis posits that surface reactions with product-like transition states are relatively structure sensitive, but reactions with reactant-like transition states are relatively insensitive to the nature of the catalyst surface.[9,18,19] This hypothesis is consistent with a number of examples for which surface transition states have been characterized in detail.[9,18–21]

In this paper, we describe DFT calculations that have been used to characterize the reaction rates and transition states for β-hydride elimination of ethyl on Cu(100), Cu(111), Cu(110), and Cu(221). We show that tunneling contributions are significant for the reaction rates on the latter three surfaces at the temperatures that are relevant for TPD experiments with these reactions. This observation means that care must be taken in comparing the reaction barriers predicted by DFT with those that come from interpreting TPD experiments. We introduce a straightforward way to address this issue based on generating simulated TPD data from rate constants developed from DFT that include tunneling corrections. When the data are examined in this way, the agreement between the reaction barriers calculated by DFT and seen in experiments is good. We have characterized the transition state for β-hydride elimination of ethyl on each surface and the reverse hydrogenation reaction, and we use this information to discuss the general hypothesis articulated above. We have also characterized the charge transfer that occurs in these transition states, which provides direct information that could previously only be accessed indirectly by experiments.

II. METHODS

We performed plane wave density functional theory calculations using the Vienna *ab initio* simulation package[22,23] (VASP) with the ultrasoft pseudopotentials available in this package.[24,25] All results below are from calculations using the PW91 generalized gradient approximation functional.[26,27] A plane wave expansion with a cutoff of 29.2 Ry was used in all calculations. Total energy calculations used the residual minimization method for electronic relaxation with Methfessel-Paxton Fermi-level smearing with a width of 0.2 eV. Geometries were relaxed using a conjugate gradient algorithm until the forces on all unconstrained atoms were less than 0.03 eV/Å. The results below are from calculations with a $5\times5\times1$ Monkhorst-Pack k-point mesh. The DFT-optimized lattice constant for Cu was found to be 3.64 Å, in good agreement with the experimental value of 3.62 Å.[28] Cu(100), Cu(110), and Cu(111) were represented by slabs five layers thick and a vacuum spacing of 11–14 Å. All calculations for these flat surfaces placed a single adsorbed molecule in a 3×3 surface unit cell. The Cu(221) surface was modeled with four stepped layers, with six atoms per layer in each unit cell and a vacuum spacing of 11 Å. One adsorbed molecule was placed in a 3×1 surface unit cell during calculations with this stepped surface. All substrate metal atoms were fixed in their bulk positions, defined using the DFT-optimized lattice constant, during our calculations.

Transition states were determined using the nudged elastic band (NEB) method, allowing full relaxation of adsorbate atoms. Reaction paths for these calculations were initially constructed by creating configurations via interpolation between the reactant and product of interest. These configurations were then manually adjusted to maintain chemically reasonable bond lengths for each bond not directly involved in the reaction. At the conclusion of each NEB calculation, the highest energy configuration was geometry optimized using a quasi-Newton method that converges to a local critical point on the potential surface.

After the converged configurations of each initial state and transition state were determined, vibrational frequencies were calculated for each state within the harmonic approximation. The Hessian matrix was calculated using finite differences based on displacements in each Cartesian coordinate of 0.02–0.03 Å. Only the vibrational modes defined by atoms in the adsorbed molecule(s) were considered in these calculations. In all cases, the initial and final states along each reaction path were found to have all positive vibrational frequencies, as expected for local minima on a potential energy surface. Each transition state was found to have exactly one imaginary vibrational frequency.

To calculate surface reaction rates, we applied harmonic transition state theory[29] (HTST) using

$$k^{\mathrm{HTST}}(T) = \nu^{\mathrm{HTST}}(T)\exp(-E_{\mathrm{ZP}}/k_B T), \tag{1}$$

$$\nu^{\mathrm{HTST}}(T) = \prod_{i=1}^{21} \nu_i^{\mathrm{IS}} \Big/ \prod_{j=1}^{20} \nu_j^{\mathrm{TS}}, \tag{2}$$

where k_B is Boltzmann's constant and E_{ZP} is the classical activation energy after zero-point (ZP) energy corrections,

$$E_{\mathrm{ZP}} = E(\mathrm{TS}) - E(\mathrm{IS}) + \sum_j \frac{h\nu_j^{\mathrm{TS}}}{2} - \sum_i \frac{h\nu_i^{\mathrm{IS}}}{2}. \tag{3}$$

Here, h is Planck's constant. In these expressions, there are $3N$ ($N=7$ for ethyl) vibrational modes for the initial state (IS), with frequencies ν_i ($i=1,2,\ldots,21$), and $3N-1$ modes for a transition state (TS), with frequencies ν_j ($j=1,2,\ldots,20$). One imaginary frequency, denoted by $\nu_{\pm}$, exists for the transition state.

It is known from hydrogen diffusion in metals and on metal surfaces that tunneling effects for hydrogen play an important role for $T<200$ K.[30–32] The experimentally observed peak temperatures for ethyl decomposition on Cu surfaces are in the range of 225–255 K, so it is possible that tunneling effects may be important in these systems. To examine this possibility, the semiclassically corrected harmonic transition state theory (SC-HTST) formulated by Fermann and Auerbach[29] was applied. The reaction constant using the Fermann-Auerbach approach is written as

$$k^{\text{SC-HTST}}(T) = k^{\mathrm{HTST}}(T)\Gamma(T), \tag{4}$$

where $k^{\mathrm{HTST}}(T)$ is the harmonic TST reaction constant defined above and $\Gamma(T)$ is the tunneling correction, which is given by

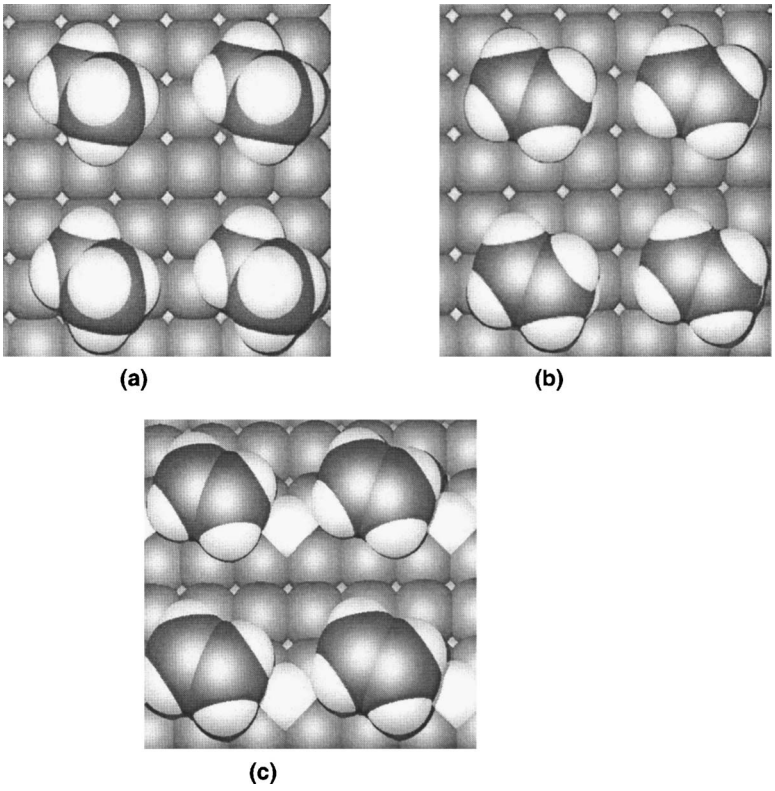

FIG. 1. Top views of the (a) initial state, (b) transition state, and (c) final state for ethyl decomposition on Cu(100). Each image shows four 3×3 surface unit cells.

$$\Gamma(T) = \frac{1+\exp(E_{ZP}/kT)}{1+\exp(2\theta_0)} + \frac{1}{2}\int_{-\infty}^{\theta_0} d\theta \,\mathrm{sech}^2\,\theta \exp\left(\frac{h\nu_{\pm}\theta}{\pi kT}\right). \quad (5)$$

In this expression, $\theta_0=(\pi E_{ZP})/(h\nu_{\pm})$.[29] One important parameter in SC-HTST is the crossover temperature, given as

$$T_c = \frac{h\nu_{\pm}E_{ZP}/k_B}{2\pi E_{ZP} - h\nu_{\pm}\ln 2}. \quad (6)$$

At temperatures lower than the crossover temperature, tunneling makes a significant contribution in Eq. (4). It is useful to note that the tunneling correction depends both on the classical activation energy for the reaction and the width of the barrier (as defined by the imaginary frequency, $\nu_{\pm}$). More sophisticated methods for including tunneling effects within diffusion or reaction rate constants are well known,[30–32] but they typically require considerably more information about the potential energy surface for the process of interest than in the Fermann-Auerbach method. The formalism above is convenient because it uses only information that is already available once HTST is applied as defined above.

Because the rates defined by Eq. (4) are more complicated than those resulting from the TST result with no tunneling corrections, it is useful to understand how these rates would be observed in TPD experiments. In TPD experiments with adsorbed ethyl groups on Cu surface, ethylene is produced via β-hydride elimination of ethyl and the ethylene desorbs immediately.[6] The DFT-calculated desorption energy of ethylene is considerably less than the activation energy for β-hydride elimination of ethyl, in qualitative agreement with experimental observations. The β-hydride elimination reaction of ethyl on Cu surfaces can, therefore, be considered to follow first-order kinetics, $r=-d\theta/dt=k\theta$, where k is the reaction constant and θ is the adsorbate coverage. This expression can be evaluated using HTST or SC-HTST. To examine the predictions of these two rate theories for TPD experiments, we numerically integrated the differential equation defined for the surface coverage using a constant heating rate $\beta=dT/dt=$const. We used a fourth-order Runge-Kutta method for this integration, with a step size of 0.01 K. Trial calculations with several other step sizes indicated that this step size gave well converged results. Because the first-order kinetics assumed by our model is coverage independent, we chose $\theta=1.0$ at $T=120$ K as the initial condition for each calculation.

III. RESULTS

A. Cu(100)

The initial state, transition state, and final state for β-hydride elimination of ethyl on Cu(100) found by DFT are shown in Fig. 1. Our calculations indicate that the bridge site is the most stable binding site for ethyl adsorption on Cu(100) with a binding energy of −1.59 eV, compared to a calculated binding energy of −1.55 eV on an atop site and −1.16 eV on a hollow site. The C—C bond in the adsorbed ethyl on a bridge site is oriented along the ⟨110⟩ direction on the surface. The initial state for the reaction was chosen to be the bridge site. It is, of course, possible that a reaction path starting from the atop site may have a lower net barrier than the path we have examined, but we have not explicitly performed calculations to examine this possibility. The product is chosen to be a coadsorption state, in which the ethylene is separated from the β-hydrogen adsorbed on a hollow site, similar to the calculations of Zhang and Hu.[33] The ethylene in the final state is found to prefer a di-σ adsorption mode rather than a π bound adsorption mode, in agreement with

TABLE I. Structural and energetic properties of adsorbates in the β-hydride elimination of ethyl on Cu(100), with energy in eV, angles in degrees, and distances in Å. $d(C_2—Cu)$ is the distance between the β-carbon and the nearest Cu atom in the top surface layer. $d(H_{ads}—Cu)$ is the distance between the β-hydrogen and the nearest Cu atom in the top layer. $d(C_1—C_2)$ is the distance between the C atom and the β-C atom. $d(C_2—H_{ads})$ is the distance between the β-hydrogen and the β-carbon. $\theta(H—C_1—H)$ is the average value of the angles between C_1 and H. The dihedral angle is defined by the HHC_1 and HHC_2 angles. The energies include zero point energy corrections.

	Ethyl (initial)	Transition state	Ethylene+H (final)
$E=E_{state}-E_{initial}$	0.0	0.76	0.12
$d(C_2—Cu)$	2.10	2.34	
$d(H_{ads}—Cu)$		1.71	1.88
$d(C_2—H_{ads})$	1.10	1.65	4.33
$d(C_1—C_2)$	1.53	1.41	1.34
$d(C_1—H)$	1.10	1.10	1.10
$d(C_2—H)$	1.10	1.10	1.10
$\theta(H—C_1—H)$	105	116	116
$\theta(H—C_1—C_2)$	109	119	122
$\theta(H—C_2—H)$	107	116	116
Dihedral $(C_2—HH—C_1)$		17.5	1.7

previous cluster and slab calculations.[34] The overall reaction is found to be endothermic, with a calculated reaction energy of 0.12 eV after zero-point energy (ZPE) corrections. The activation energy barrier of this reaction is 0.76 eV after ZPE corrections. If ZPE corrections are not included, a considerably higher barrier of 0.91 eV is found. The geometries of the initial state, transition state, and final state are listed in Table I.

B. Cu(111)

The most stable binding site for ethyl on Cu(111) is found to be an atop site with a binding energy of −1.34 eV, compared to a slightly less favorable binding energy of −1.31 eV on a bridge site and −1.23 eV on a hollow site. These observations are consistent with previous DFT studies of ethyl adsorption on this surface.[11] In its most stable configuration, the C—C bond in the adsorbed ethyl is oriented along the ⟨110⟩ direction on the surface. The initial state for the reaction was chosen to be the most stable configuration binding on an atop site. Michaelides and Hu have previously used DFT to study the decomposition of methyl on several closed packed surfaces including Pt(111), Cu(111), and Ni(111).[15] The choice of the final state in our work is similar to their studies, in which the eliminated β-hydrogen is adsorbed on a hollow site spatially separated from the adsorbed ethylene. The overall reaction is found to be endothermic, with a calculated reaction energy of 0.10 eV (0.21 eV) after (before) ZPE corrections. The activation energy for the reaction, including zero-point energies, was calculated to be 0.69 eV. Table II summarizes the geometries of the reactant, transition state, and final state.

C. Cu(110)

There are more binding sites on the relatively open Cu(110) surface than on the more closely packed Cu(100) and Cu(111) surfaces. Two distinct bridge sites were considered in our calculations. The short bridge site is found to be the most stable binding sites for ethyl adsorption on Cu(110) with a binding energy of −1.78 eV, compared to a calculated binding energy of −1.61 eV on an atop site. The hollow site and the long bridge site are not stable binding sites. Configurations that began at hollow or long bridge sites ultimately converged to the configuration with C bonded to a short bridge site. In its most stable configuration, the C—C bond in the adsorbed ethyl is oriented along the ⟨100⟩ direction on the surface. In our calculations for the reaction, we chose the initial state to be the most stable configuration binding on a short bridge site. As for Cu(100) and Cu(111), the final state was defined by spatially separating ethylene and atomic H in their preferred binding configurations. Previous DFT studies showed that two stable H adsorption sites exist on Ni(110), a pseudo-three-fold hollow site and the long bridge site.[35] We examined both of these configurations for H adsorption on Cu(110) and found that the pseudo-three-fold site is the most favored, in agreement with the result on Ni(110).[35] The overall reaction is found to be endothermic, with calculated reaction energy of 0.16 eV after ZPE corrections. The activation energy barrier of this reaction was calculated to be 0.65 eV when including zero-point energies (0.81 eV if these energies are not included). An alternative reaction path connecting the same initial state with a different final state adsorbing hydrogen on a long bridge site was also examined and was found to have a zero-point energy corrected activation energy of 0.84 eV. Our discussion in the remainder of the paper is restricted to the reaction path with the lower activation energy. The geometries of the adsorbates during the reaction along this path are summarized in Table III.

TABLE II. Structural and energetic properties of adsorbates in the β-hydride elimination of ethyl on Cu(111). The notation is similar to Table I.

	Ethyl (initial)	Transition state	Ethylene+H (final)
$\Delta E=E_{state}-E_{initial}$	0	0.69	0.10
$d(C_2—Cu)$	2.08	2.37	
$d(H_{ads}—Cu)$		1.77	1.76
$d(C_2—H_{ads})$	1.1	1.58	4.40
$d(C_1—C_2)$	1.52	1.42	1.35
$d(C_1—H)$	1.1	1.09	1.1
$d(C_2—H)$	1.1	1.09	1.10
$\theta(H—C_1—H)$	106	115	116
$\theta(H—C_1—C_2)$	109	119	121
$\theta(H—C_2—H)$	107	115	116
Dihedral $(C_2—HH—C_1)$		20.4	2.0

D. Cu(221)

The Cu(221) surface is composed of (111) terraces separated by (110) step edges. We considered several possible configurations for ethyl adsorption, including adsorption above the step edge on the terrace. Previous DFT studies have shown that the step edges can enhance the adsorption energies of alkyls.[36] Our results are consistent with this observation; we find that ethyl prefers to adsorb on top of the step edge with a binding energy of −1.80 eV, compared to a

TABLE III. Structural and energetic properties of adsorbates in the β-hydride elimination of ethyl on Cu(110). The notation is similar to Table I.

	Ethyl (initial)	Transition state	Ethylene+H (final)
$\Delta E = E_{state} - E_{initial}$	0.0	0.65	0.16
$d(C_2—Cu)$	2.14	2.12	
$d(H_{ads}—Cu)$		1.71	1.83
$d(C_2—H_{ads})$	1.1	1.54	4.77
$d(C_1—C_2)$	1.53	1.43	1.35
$d(C_1—H)$	1.1	1.1	1.1
$d(C_2—H)$	1.1	1.1	1.1
$\theta(H—C_1—H)$	102	115	116
$\theta(H—C_1—C_2)$	107	120	122
$\theta(H—C_2—H)$	102	115	116
Dihedral $(C_2—HH—C_1)$		17.5	1.7

TABLE IV. Structural and energetic properties of adsorbates in the β-hydride elimination of ethyl on Cu(221). The notation is similar to Table I.

	Ethyl (initial)	Transition state	Ethylene+H (final)
$\Delta E = E_{state} - E_{initial}$	0.0	0.66	0.13
$d(C_2—Cu)$	2.00	2.12	
$d(H_{ads}—Cu)$		1.66	1.74
$d(C_2—H_{ads})$	1.10	1.66	4.87
$d(C_1—C_2)$	1.52	1.42	1.36
$d(C_1—H)$	1.10	1.09	1.09
$d(C_2—H)$	1.10	1.09	
$\theta(H—C_1—H)$	107	114	116
$\theta(H—C_1—C_2)$	108	120	121
$\theta(H—C_2—H)$	107	115	116
Dihedral $(C_2—HH—C_1)$		17.5	5.6

calculated binding energy of −1.41 eV on an atop site in the terrace and a binding energy of −1.65 eV on an atop site near the step in the terrace. We only computed a reaction path for the reaction where the initial state is an ethyl on top of the step edge. The product state was chosen to be the coadsorption state in which the ethylene is separated from the hydrogen adsorbed on a hollow site on the (111) terrace, as in the DFT study of methyl[12] of Ciobica *et al.* and the work of Chen *et al.* on methoxy.[36] Ethylene is found to prefer to adsorb at the top of the step edges on Cu(221). The configurations determined using DFT for the reaction path that we considered are shown in Fig. 2. The overall reaction is found to be endothermic, with calculated reaction energy of 0.13 eV after ZPE corrections. The activation energy barrier of this reaction was found to be 0.66 eV after ZPE corrections (0.83 eV if these corrections are not included). The calculated geometries of the adsorbates during the reaction are listed in Table IV.

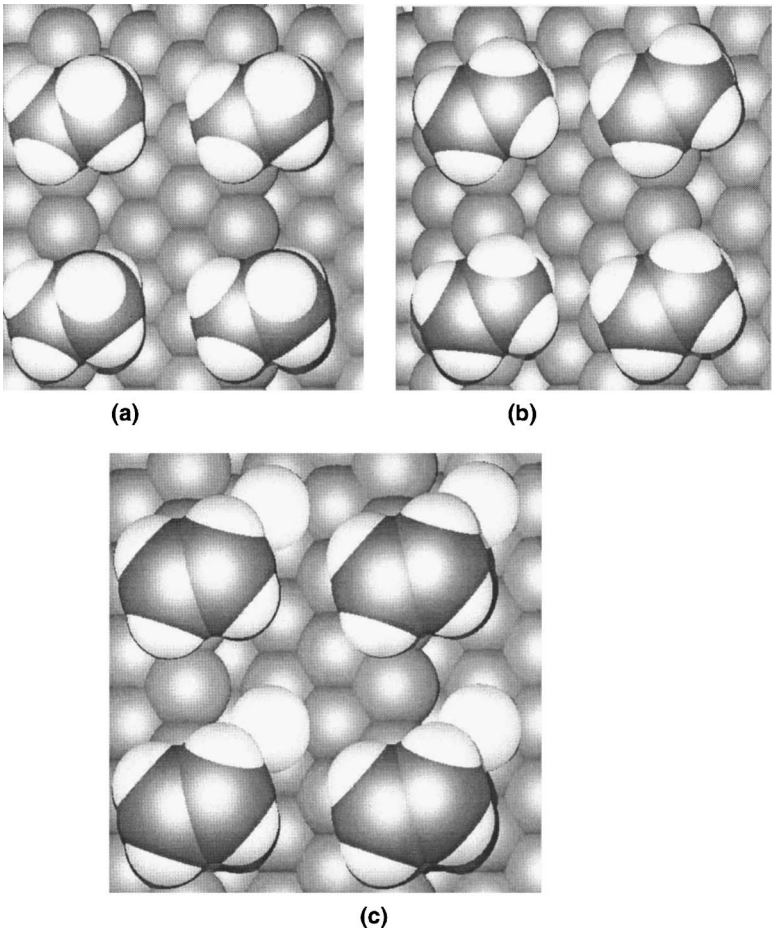

FIG. 2. Top views of the (a) initial state, (b) transition state, and (c) final state for ethyl decomposition on Cu(221). The step edges are oriented from the bottom to top of each image.

TABLE V. Calculated and observed TPD peak temperature for β-hydride elimination of ethyl on the surfaces indicated, with all temperatures in K. Each entry lists the results for a heating rate of 4 K/s (2 K/s). Experimental data for heating rates of 2 K/s are from Sung and Gellman (Ref. 10), while data for heating rates of 4 K/s are from Jenks *et al.* (Ref. 6).

	Cu(100)	Cu(111)	Cu(110)	Cu(221)
TST, $\nu=10^{13}$ s^{-1}	286 (280)	261 (257)	246 (241)	250 (244)
HTST with DFT prefactors	286 (280)	262 (256)	245 (240)	237 (234)
HTST with tunneling	286 (280)	240 (232)	218 (201)	212 (197)
Experimental data	255 (N/A)	247 (247)	225 (N/A)	N/A (226)

TABLE VI. Effective activation barriers determined from DFT calculations and observed in TPD experiments for a heating rate of 4 K/s (2 K/s). All energies are in eV. Experimental data for heating rates of 4 K/s are from Sung and Gellman (Ref. 10), while data for heating rates of 2 K/s are from Jenks *et al.* (Ref. 6).

	Cu(100)	Cu(111)	Cu(110)	Cu(221)
DFT	0.74 (0.74)	0.63 (0.63)	0.57 (0.54)	0.56 (0.53)
Experiment	0.66 (N/A)	0.64 (0.64)	0.58 (N/A)	N/A (0.61)

IV. DISCUSSION

A. Comparison with experimental results

To compare our results with observations of β-hydride elimination of ethyl made using TPD, we first need to determine whether tunneling corrections may influence this comparison. The tunneling crossover temperatures predicted by our calculations using Eq. (6) are 155, 228, 220, and 213 K for Cu(100), Cu(111), Cu(110), and Cu(221), respectively. Because the experimentally observed TPD peak temperatures for these reactions range from 220 to 250 K, this initial calculation suggests that tunneling may influence the experimental results except perhaps on Cu(100).

We simulated TPD spectra for each surface as described in Sec. II with three approaches. First, we used transition state theory using the zero-point energy activation energies calculated with DFT, but assuming that the prefactor defining the reaction rate was 10^{13} s^{-1}. This approach is of interest because experimental TPD spectra are often analyzed by making this assumption about the reaction rate constant prefactor. Second, we used HTST with the prefactors defined via our DFT calculations. Third, we used HTST with the DFT-derived prefactors and with tunneling corrections. We view this third approach as the most accurate of the three methods. The peak temperatures calculated with each of these methods are listed for two different surface heating rates in Table V.

Table V shows that including tunneling corrections makes an appreciable difference to the calculated TPD peak temperatures on all the surfaces we considered except Cu(100). This is consistent with the crossover temperatures listed above. For the other three surfaces, including the tunneling corrections lowers the calculated peak temperatures by up to 40 K. An obvious implication of these results is that the observed peak temperatures would be significantly different if deuterated reactants were used. We are unaware of any experimental data from experiments of this type for the Cu surfaces we have considered here.

The contributions of tunneling to several of the reactions we have studied make direct comparisons between the activation energies computed with DFT and those inferred from TPD spectra problematic. One way to resolve this issue is to simulate TPD spectra using the tunneling corrected HTST rate constants determined from DFT and then to analyze these spectra in the same way as the available experimental data. Specifically, we apply the Redhead equation to our simulated spectra while assuming that the reaction prefactor is 10^{13} s^{-1}. This procedure gives an effective activation energy barrier for each reaction. These barriers are listed in Table VI together with the available experimental data. The agreement between the experimental observations and our DFT results is good. For Cu(111) and Cu(110), our calculated effective activation energies are essentially identical to the experimental results. On Cu(100), the DFT result is 0.08 eV larger than the experimental observation, while on Cu(221), the DFT result is 0.08 eV smaller than the experimental result.

The main message from the results in Tables V and VI is not that including tunneling corrections in our DFT-based calculations improves the agreement between these calculations and experimental observations. Systematic uncertainties between our DFT-computed activation energies and the results from the true potential energy surface exist simply because of the approximations inherent in DFT. Instead, the key observation from our DFT results is that inclusion of tunneling changes the interpretation of the TPD peak temperatures in ways that have directly observable implications for experimental measurements. The obvious strategy to explore this issue in a way that avoids the uncertainties mentioned above is to perform experiments for these systems using deuterated species.

B. Characterization of transition states

One useful way to compare groups of transition states is to classify them as being either late (that is, product-like) or early (reactant-like). The labels for these situations already indicate that this classification is, at best, qualitative. One way to classify the transition states in the reaction paths described above is to examine the C—C bond distance during the reaction. We denote the change in this distance between the initial state and the transition state by $\Delta\vec{d}_{C—C}$. From Tables I–IV, we see that $-0.12 \leq \Delta\vec{d}_{C—C} \leq -0.10$ Å. Considering the reverse reactions in the same way, the change in the C—C bond distance between the final state and the transition state is $0.06 \leq \Delta\vec{d}_{C—C} \leq 0.08$ Å. This suggests that the transition states are more product-like than reactant-like, although by this measure they certainly contain characteristics of the reactants. This classification is less clear-cut than a similar analysis of fluorinated ethoxy decomposition in our previous work.[21,37] In that case, $-0.17 \leq \Delta\vec{d}_{C—O} \leq -0.13$ Å and $0.05 \leq \Delta\vec{d}_{C—O} \leq 0.08$ Å. Another means of characteriz-

TABLE VII. Bader charge differences between species in the TS and IS on Cu surfaces, with δ(atom) =Bader charge of atom in TS−bader charge of atom in IS, δ(molecule) =Σ(bader charge of molecular atoms in TS)−Σ(bader charge of molecular atoms in IS), and δ(surfaces) =Σ(bader charge of surface atoms in TS)−Σ(bader charge of surface atoms in IS).

Surface	$\delta(C_1)$	$\delta(C_2)$	$\delta(H_\beta)$	δ(molecule)	δ(surface)	E_{act}
Cu(111)	−0.100	0.020	0.250	−0.02	0.02	0.69
Cu(100)	−0.213	0.067	0.169	−0.04	0.04	0.76
Cu(110)	−0.101	0.107	0.050	−0.07	0.07	0.65
Cu(221)	−0.004	0.266	0.044	0.00	0.00	0.66

ing the transition states is to examine changes in the bond angles that do not directly participate in the reaction. Tables I–IV show that in every case, θ(H—C_1—H) and θ(H—C_2—H) change distinctly along the reaction path and, more importantly, are essentially identical in the transition state and final state. Considering the bond length and bond angle changes together, we can characterize the transition states for the β-hydride reactions we have examined as weakly product-like.

To characterize charge transfer during the reactions, we computed the Bader charges on individual atoms in each initial state and transition state. The net charge differences observed in each reaction are summarized in Table VII. The overall trend is that a small amount of charge is transferred from the reacting molecule to the substrate Cu surfaces during the reactions except on stepped Cu(221). The Bader charge (in units of electron charge) on both the β-C_2 and the β-H increases during the reactions. All the transition states can be schematically described as $C^{\delta+}$—$C^{\delta-}\cdots H^{\delta-}$ with respect to the initial state. This differs from previous experimental interpretations of the transition state having the form $C^{\delta+}\cdots H^{\delta-}$ with respect to the initial state in β-hydride elimination of alkyls on metal surfaces.[2] On the flat surfaces, the C_1 atom often possesses more charge in absolute value than β-C_2, although on Cu(110) they carry almost the same charges. On the stepped Cu(221) surface, there is no net transfer of electrons from the molecule to the surface during the reactions. In the current reactions on flat surfaces, we note that the results arise from the delocalization effect of the C=C double bond during the reaction, as Truhlar and Morokuma concluded in their work on ethyl on Pd(111).[16]

C. Hypotheses regarding structure sensitivity

As described in Sec. I, one general hypothesis regarding the structure sensitivity of surface reactions is that reactions with product-like transition states are less structure sensitive than reactions with reactant-like transition states.[9,18,19] We can use our DFT results to examine this hypothesis by noting that since we have classified the transition states for β-hydride elimination as (weakly) product-like, then the reverse reactions must be characterized as having reactant-like transition states. Figure 3 shows the zero-point energy corrected activation energies for each forward and reverse reaction that we considered with DFT. The activation energies for the forward reactions are also listed in Table I–IV. The activation energies for the reverse reactions were calculated to be 0.64, 0.59, 0.49, and 0.53 eV on Cu(100), Cu(111), Cu(110), and Cu(221), respectively. The barriers for the forward reactions vary by 0.09 eV among the four surfaces, while the variation in the reverse reaction barriers is 0.15 eV. This does not contradict the hypothesis above, since the hypothesis does not predict whether a given reaction will show strong structure sensitivity, but only which direction in a reaction will be more structure sensitive. In situations such as the one we have examined where the reaction is at most weakly structure sensitive in either direction, the hypothesis above has only a limited predictive ability.

Some readers may note that if the effective reaction barriers listed in Table VI are used to characterize the forward reactions, then the reaction barriers vary by 0.21 eV among the four surfaces, a range considerably larger than the range for the barriers to the reverse reaction shown in Fig. 3. This comparison is not entirely appropriate, since the effective energy barriers in Table VI were calculated from simulated TPD spectra that include tunneling contributions, while the barriers for the reverse reaction in Fig. 3 are simply the zero-point energy corrected DFT barriers. Much of the variation in the TPD-derived barriers arises because tunneling contributions play an important role on Cu(111), Cu(110), and Cu(221) but not on Cu(100).

Our results also make it possible to examine a general rule proposed by Liu and Hu regarding the location of catalytic reactions on metal surfaces.[38] On the basis of DFT calculations for C—H and C—O bond breaking and formation, Liu and Hu suggested that defects such as steps are always favored for dissociation reactions. In a way, our results for ethyl decomposition on Cu(221) support this idea, since the reaction barrier when the reaction occurred near the

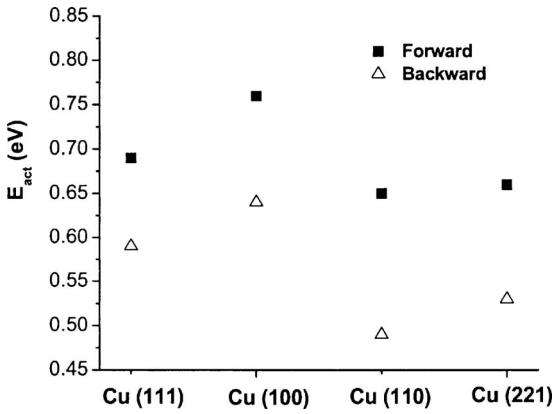

FIG. 3. Activation energy barriers computed using DFT for forward (filled squares) and backward (open triangles) reaction of β-hydride elimination of ethyl on four Cu surfaces, with energies in eV.

step edge was smaller than the barrier on the terrace [as characterized by our results for Cu(111)]. This concept breaks down, however, if the reaction rate on polycrystalline Cu is considered. Our results are in agreement with experimental findings that the reaction rates for ethyl decomposition on Cu(110) and Cu(221) are very similar. Note that the step on the Cu(221) surface has the structure of a (110) microfacet projecting out of the (111) terrace, and so similarities between the two might be expected. We also found that the binding energies of ethyl are very similar on these two surfaces. On the surface of polycrystalline Cu, the surface area of Cu(110) will typically be much larger than the area covered by step edges like that on Cu(221) that are defined by (111)-oriented terraces. This means that the overall reaction rate for ethyl decomposition on these two regions of the crystal will be dominated by reactions on the flat Cu(110) surface, contrary to the rule suggested by Liu and Hu. In this context, it is important to point out that various other structurally distinct surface steps can occur on Cu surfaces as the identity of the terrace and the orientation of the step are varied.[39] It is conceivable that the reaction rate for ethyl decomposition on one of the other step types that has not yet been examined by experiment or our calculations could be much faster than on Cu(110) or Cu(221). If this is the case, then the proposed rule of Liu and Hu could correctly describe the properties of polycrystalline Cu.

V. CONCLUSION

We have used plane wave DFT calculations to study the reaction rates and surface transition states for ethyl decomposition on Cu(100), Cu(111), Cu(110), and Cu(221). Our results are in agreement with the conclusion of previous experiments that the reaction rates for this process on the flat Cu(110) surface and on the stepped Cu(221) surface are similar. An interesting feature of these reactions is that at the temperatures that are relevant for observing the reaction with TPD experiments, tunneling contributions to the reaction rate are significant. We used a semiclassically corrected version of harmonic transition state theory (HTST) that predicts these tunneling contributions using only the information that is necessary for classical HTST. The importance of tunneling contributions complicates the interpretation of experimental TPD spectra, since the usual approach of applying the Redhead equation assuming a constant preexponential factor is not accurate. We showed, by interpreting simulated TPD spectra based on our DFT-based reaction rates in the same way as earlier experiments, that the effective activation energy barriers for ethyl decomposition on these Cu surfaces from our DFT calculations are in good agreement with experimental observations.

The fact that ethyl decomposition is only weakly structure sensitive on the Cu surfaces we have studied makes this reaction a challenging one to consider within the general frameworks that have been proposed to describe reactions of this type. One proposition of this type is that surface reactions with product-like transition states are more structure sensitive than reactions with reactant-like transition states. The transition states found in our DFT calculations can be described as more product-like than reactant-like, but the geometry of the transition states includes both product-like and reactant-like features. The observed structure sensitivity is not inconsistent with the proposition above, but it is perhaps not reasonable to expect such an idea to be able to predict differences in reaction energetics as small as those that occur between β-hydride elimination of ethyl on the different Cu surfaces and the reverse reaction. Our results also illustrate an example where it is not necessarily possible to classify the transition states as simply product-like or reactant-like with absolute clarity.

ACKNOWLEDGMENTS

This work was supported by the Donors of the American Chemical Society Petroleum Research Fund.

[1] R. Alcala, J. Greeley, M. Mavrikakis, and J. A. Dumesic, J. Chem. Phys. **116**, 8973 (2002).
[2] J. G. Forbes and A. J. Gellman, J. Am. Chem. Soc. **115**, 6277 (1993).
[3] X. Q. Gong, R. Raval, and P. Hu, J. Chem. Phys. **122**, 024711 (2005).
[4] F. Zaera, Isr. J. Chem. **38**, 293 (1998).
[5] F. Zaera, Chem. Rev. (Washington, D.C.) **95**, 2651 (1995).
[6] C. J. Jenks, B. E. Bent, and F. Zaera, J. Phys. Chem. B **104**, 3008 (2000).
[7] C. J. Jenks, B. E. Bent, and F. Zaera, J. Phys. Chem. B **104**, 3017 (2000).
[8] A. J. Gellman and Q. Dai, J. Am. Chem. Soc. **115**, 714 (1993).
[9] A. J. Gellman, Curr. Opin. Solid State Mater. Sci. **5**, 85 (2001).
[10] D. Y. Sung and A. J. Gellman, Surf. Sci. **551**, 59 (2004).
[11] G. C. Wang, J. Li, X. F. Xu, R. F. Li, and J. Nakamura, J. Comput. Chem. **26**, 871 (2005).
[12] I. M. Ciobica, F. Frechard, R. A. Santen, A. W. Kleyn, and J. Hafner, J. Phys. Chem. B **104**, 3364 (2000).
[13] A. Michaelides and P. Hu, J. Chem. Phys. **112**, 8120 (2000).
[14] A. Michaelides and P. Hu, J. Am. Chem. Soc. **122**, 9866 (2000).
[15] A. Michaelides and P. Hu, J. Chem. Phys. **114**, 2523 (2001).
[16] D. G. Truhlar and K. Morokuma, ACS Symp. Ser. **721**, 226 (1998).
[17] I. Kovacs and F. Solymosi, J. Phys. Chem. **97**, 11056 (1993).
[18] A. J. Gellman, Acc. Chem. Res. **33**, 19 (2000).
[19] A. J. Gellman, J. Phys. Chem. B **106**, 10509 (2002).
[20] A. J. Gellman, M. Buelow, and S. C. Street, J. Phys. Chem. A **104**, 2476 (2000).
[21] X. Li, A. J. Gellman, and D. S. Sholl, Surf. Sci. Lett. **600**, L25 (2006).
[22] G. Kresse and J. Hafner, Phys. Rev. B **47**, 558 (1993).
[23] G. Kresse and J. Furthmuller, Phys. Rev. B **54**, 11169 (1996).
[24] J. M. Bonello and R. M. Lambert, Surf. Sci. **498**, 212 (2002).
[25] R. L. Toomes, J.-H. Kang, D. P. Woodruff, M. Polcik, M. Kittel, and J.-T. Hoeft, Surf. Sci. **522**, L9 (2003).
[26] J. P. Perdew, J. A. Chevary, S. H. Vosko, K. A. Jackson, M. R. Pederson, D. J. Singh, and C. Fiolhais, Phys. Rev. B **46**, 6671 (1992).
[27] J. A. White and D. M. Bird, Phys. Rev. B **50**, 4954 (1994).
[28] D. R. Lide and E. H. I. R. Frederikse, *CRC Handbook of Chemistry and Physics* (CRC, New York, 2002).
[29] J. T. Fermann and S. M. Auerbach, J. Chem. Phys. **112**, 6787 (2000).
[30] B. Bhatia and D. S. Sholl, Phys. Rev. B **72**, 224302 (2005).
[31] P. G. Sundell and G. Wahnström, Phys. Rev. Lett. **92**, 155901 (2004).
[32] G. Kallen and G. Wahnström, Phys. Rev. B **65**, 033406 (2001).
[33] C. J. Zhang and P. Hu, J. Chem. Phys. **116**, 322 (2002).
[34] M. Neurock and R. A. Van Santen, J. Phys. Chem. B **104**, 11127 (2000).
[35] B. Bhatia and D. S. Sholl, J. Chem. Phys. **122**, 204707 (2005).
[36] Z. X. Chen, K. H. Lim, K. M. Neyman, and N. Rosch, J. Phys. Chem. B **109**, 4568 (2005).
[37] X. Li, A. J. Gellman, and D. S. Sholl, J. Mol. Catal. A: Chem. **228**, 77 (2005).
[38] Z. P. Liu and P. Hu, J. Am. Chem. Soc. **125**, 1958 (2003).
[39] D. S. Sholl, A. Asthagiri, and T. D. Power, J. Phys. Chem. B **105**, 4771 (2001).